# A 96 GHz Oscillator by High-Q Differential Transmission Line loaded with Complementary Split Ring Resonator in 65nm CMOS

Wei Fei, *Student Member, IEEE,* Hao Yu, *Member, IEEE,* Yang Shang, *Student Member, IEEE,* Deyun Cai, *Student Member, IEEE,* and Junyan Ren, *Member, IEEE*

***Abstract*—A 96GHz CMOS oscillator is demonstrated in this paper with the use of a high-Q metamaterial resonator. The proposed metamaterial resonator is constructed by a differential transmission-line (T-line) loaded with complementary split-ring-resonator (CSRR) engraved on the T-line. A negative real-part of permittivity (ε) is observed near the resonance frequency, which introduces a sharp stop-band and thus leads to a high-Q resonance. This paper is the first in literature to explore CMOS on-chip metamaterial resonator for oscillator design at millimeter-wave frequency region. Compared to the existing oscillators with LC-tank based resonator at around 100GHz, the proposed 96GHz oscillator with high-Q metamaterial resonator shows much lower phase noise of -111.5 dBc/Hz at 10MHz offset and FOM of -182.4 dBc/Hz.**

***Index Terms*—Metamaterial, high-Q CSRR oscillator, millimeter wave integrated circuit, 65nm CMOS.**

## I. Introduction

As CMOS technology scales down with the maximum frequency exceeding 100GHz, implementation of CMOS integrated circuits (ICs) has become feasible at millimeter (MM)-wave band, such as V-band 60GHz high-data-rate communication system [1], E-band car-radar system [2] and W-band imaging system [3]. However, as frequency pushes up, it is increasingly difficult to maintain the similar performance for various circuit blocks. Among these, phase noise performance of oscillators affects the overall system performance such as Bit Error Rate (BER) and hence is one of the primary design targets. It is well-known that Q-factor of resonators affects the phase noise of oscillators. Unfortunately, the phase noise performance for the traditional LC-tank based resonator is limited by low-Q on-chip inductor and capacitor in the MM-wave region [4]. The recent explorations of the metamaterial resonator show that split-ring-resonator (SRR) and complementary split-ring-resonator (CSRR) can exhibit high-Q factor at MM-wave frequency region.

Manuscript received June 14, 2012. This work was sponsored by NRF 2010NRF-POC001-001 and MOE TIER-1 RG26/10 grants from Singapore.



Wei Fei, Yang Shang, Hao Yu, and Kiat Seng Yeo are with the School of Electrical and Electronic Engineering, Nanyang Technological University, 50 Nanyang Ave., Singapore 639798 (phone: 65-67904509; email: haoyu@ntu.edu.sg).

Deyun Cai and Junyan Ren are with the State Key Laboratory of ASIC and System, Fudan University, Shanghai, P. R. China.

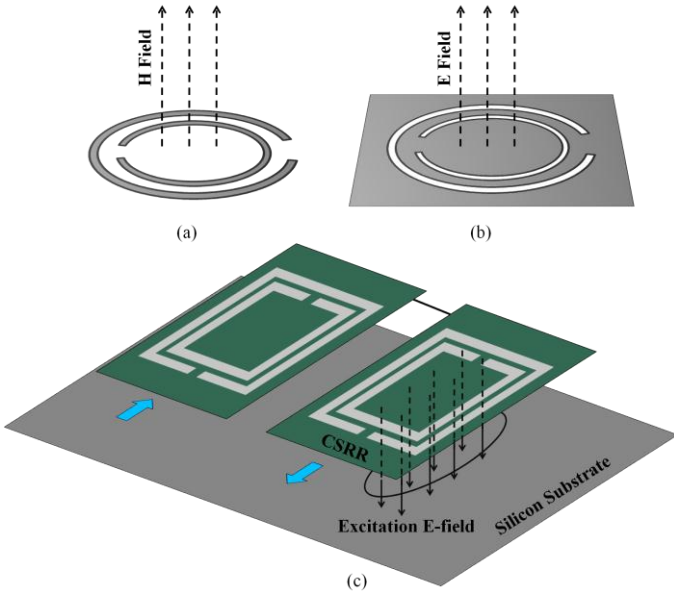


Fig. 1. (a) SRR excitation by H-field; (b) CSRR excitation by E-field; and (c) the proposed on-chip differential T-line loaded with CSRR.

Metamaterial was first demonstrated by [5] with the use of SRR and metallic wire, among which SRR shows the property of negative real-part of permeability (μ) at the resonance frequency. The planar SRR structure can be considered as a magnetic dipole excited by the magnetic field (H-Field) along the ring axis as shown in Fig. 1(a). At the same time, as the dual counterpart of SRR, CSRR shown in Fig. 1(b) was proposed by [6] based on the well-known complementary theory. CSRR shows the metamaterial property of negative real-part of permittivity (ε) at resonance frequency, and can be considered as an electric dipole excited by the electric field (E-Field) along the ring axis. Both SRR and CSRR can be deployed as the load for a host such as a transmission-line (T-line) to build metamaterial based resonators. Due to the single-negative property of SRR and CSRR, a sharp stop-band is formed at the vicinity of resonance. As such, the propagating wave at the host T-line is perfectly reflected backward with an established standing-wave. Therefore, the EM energy can be well stored

with low-loss transferring between the host and load. As a result, it provides a high-Q performance for the resonator.

There are some initial works explored for SRR or CSRR based oscillator design in PCB scale at 5.5 ~ 5.8GHz [7, 8]. Since the device feature size is inversely proportional to the operation frequency, the size of SRR or CSRR thereby becomes compact enough for on-chip implementation at high frequency region. Recently, metamaterial was explored for on-chip CMOS applications in MM-wave region due to its reduced size and loss [4, 9]. In [4], a SRR-based resonator was studied at 80GHz using CMOS 65nm process.

In this work, we are the first to demonstrate the CSRR-metamaterial based resonator for CMOS on-chip oscillator design with MM-wave integrated circuit applications [4, 6-9]. A high-Q metamaterial resonator structure is introduced at 96GHz with the use of a differential T-line loaded with CSRRs. The chip is fabricated in 65nm CMOS technology (STM 7-metal-layer). Measurements show the-state-of-art phase noise of -111.5dBc/Hz (@10MHz offset) and FOM of -182.4dBc/Hz. The rest of this paper is organized as follows. Section II presents the high-Q metamaterial resonator design, with 96GHz CMOS oscillator for demonstration in Section III. The measurement results are shown and analyzed in Section IV, and the paper is concluded in Section V.

## II. On-Chip CSRR Metamaterial Resonator

One recent CSRR design was implemented at PCB level with a microstrip T-line on the top layer as the signal line, and an engraved CSRR plane is on the bottom layer as the ground [6]. The CSRR is constructed by engraving ring-shaped holes on the metal plane, with each ring split by a small gap. The engraved CSRR then couples with microstrip T-line through an E-field to generate a negative Re(ε) feature. However, it is not feasible to implement such an engraved CSRR-ground for CMOS on-chip circuits due to the lossy substrate and thin metal layer near substrate, both of which can cause significant loss. To have a low-loss and high-Q implementation for CMOS on-chip CSRR based metamaterial resonator, a new topology is proposed in this paper. As shown in Fig. 1(c), instead of engraving CSRRs on the ground plane, they are engraved directly on metal layer using signal lines. Compared with the previous method [6], the proposed topology can realize a much stronger coupling between T-line and CSRR since they are on the same metal layer. More energy can thereby be stored in the resonator, which in turn results in a higher Q-factor.

### A. Metamaterial T-line based resonators

The metamaterial property for T-lines loaded with both SRR and CSRR can be analysed by a loaded T-line model. As shown in Fig. 2(a), a T-line can be modelled as a cascaded array of unit-cells, with equivalent circuit for each unit-cell represented by a serial per-unit length impedance ($Z$) and a parallel per-unit length admittance ($Y$). Based on theory in [10], the permeability (μ) and permittivity (ε) can be related to $Z$ and $Y$ at frequency ω by following equations:

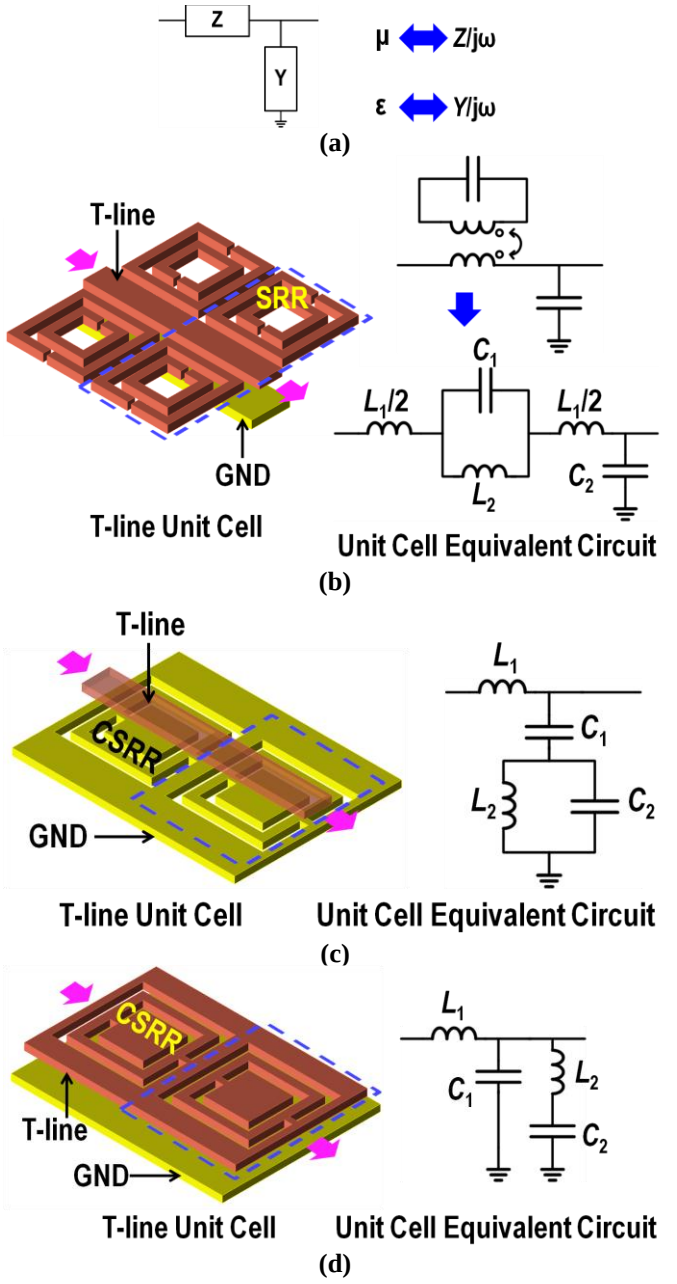


Fig. 2. Metamaterial resonators constructed by T-line loaded with SRR/CSRR: (a) T-line model, (b) T-line loaded with SRR, (c) T-line loaded with CSRR, and (d) on-chip implementation for T-line loaded with CSRR.

$$\mu = \frac{Z}{j\omega}, \varepsilon = \frac{Y}{j\omega}. \quad (1)$$

Traditional metamaterial T-lines loaded with SRR and CSRR have the layout structures and the according equivalent circuits shown in Fig. 2(b) and (c), respectively. Here $C_1$, $C_2$, $L_1$, and $L_2$ are per-unit length capacitance and inductance which determine the metamaterial property of SRR and CSRR resonators.

For T-line loaded with SRR (Fig. 2(b)), $L_1$ and $C_2$ come from T-line, while $C_1$ and $L_2$ come from magnetic coupling of SRR on both sides of T-line. The calculation $\varepsilon = \frac{Y}{j\omega} = C_2$ gives a positive real-part, while $\mu = \frac{Z}{j\omega} = \frac{L_1+L_2-\omega^2 C_1 L_1 L_2}{1-\omega^2 C_1 L_2}$.

It can be observed that when

$$\sqrt{\frac{1}{C_1 L_2}} < \omega < \sqrt{\frac{L_1+L_2}{C_1 L_1 L_2}}, \quad (2)$$

Re(μ) is negative and Re(ε) is positive. Note that magnetic plasma is formed, where propagating waves become evanescent waves [11]. As a result, energy cannot propagate through the resonator and is perfectly reflected back to establish a standing-wave. This becomes the physical foundation of SRR-metamaterial based resonator.

Similarly, for T-line loaded with CSRR (Fig. 2(c)), $L_1$ comes from T-line, while $C_1$, $C_2$, and $L_2$ come from electric coupling of CSRR on the ground. When

$$\sqrt{\frac{1}{(C_1+C_2)L_2}} < \omega < \sqrt{\frac{1}{C_2 L_2}}, \quad (3)$$

*Z* is positive and *Y* is negative, which leads to a positive Re(μ) and a negative Re(ε). In this case, electric plasma is formed, where propagating waves also become evanescent waves [11]. As a result, energy cannot propagate through the resonator and is perfectly reflected back to establish a standing-wave. This becomes the physical foundation of CSRR-metamaterial based resonator. Note that T-line loaded with CSRR has the advantage of more compact area over T-line loaded with SRR. However, the previous approach [6] by engraved CSRR-ground cannot be done on-chip due to high loss.

### *B. Proposed new CSRR T-line based resonator*

The proposed new topology in Fig. 1(c) is able to solve this problem by reducing the substrate loss while maintaining its metamaterial property. As analysed in Fig. 2(d), $L_1$ and $C_1$ come from T-line, while $L_2$ and $C_2$ come from electric coupling of CSRR on T-line. When

$$\sqrt{\frac{1}{C_2 L_2}} < \omega < \sqrt{\frac{C_1+C_2}{C_1 C_2 L_2}}, \quad (4)$$

*Z* is positive and *Y* is negative, which gives a positive Re(μ) and a negative Re(ε). As a result, electric plasma is created and a CSSR-metamaterial based resonator is thus formed.

Moreover, the proposed topology in Fig. 1(c) deploys a differential structure, which provides a compact area, puts both inputs on the same side, provides an AC ground for easy DC supply, and further reduces coupling to lossy ground/substrate, thus improving the Q-factor eventually.

The metamaterial property of the proposed CSRR-metamaterial based resonator and its high-Q feature is also validated through simulation. Note that the metamaterial property can be calculated from S-parameters using following equations [12]:

$$n = \frac{1}{kd}\cos^{-1}\left[\frac{1-S_{11}^2+S_{21}^2}{2S_{21}}\right], z = \sqrt{\frac{(1+S_{11})^2-S_{21}^2}{(1-S_{11})^2-S_{21}^2}},$$
$$\varepsilon = \frac{n}{z}, \mu = nz. \quad (5)$$

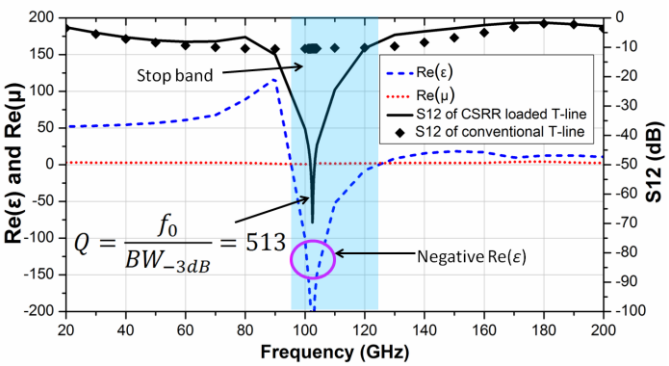


Fig. 3. EM characterization of the proposed metamaterial resonator.

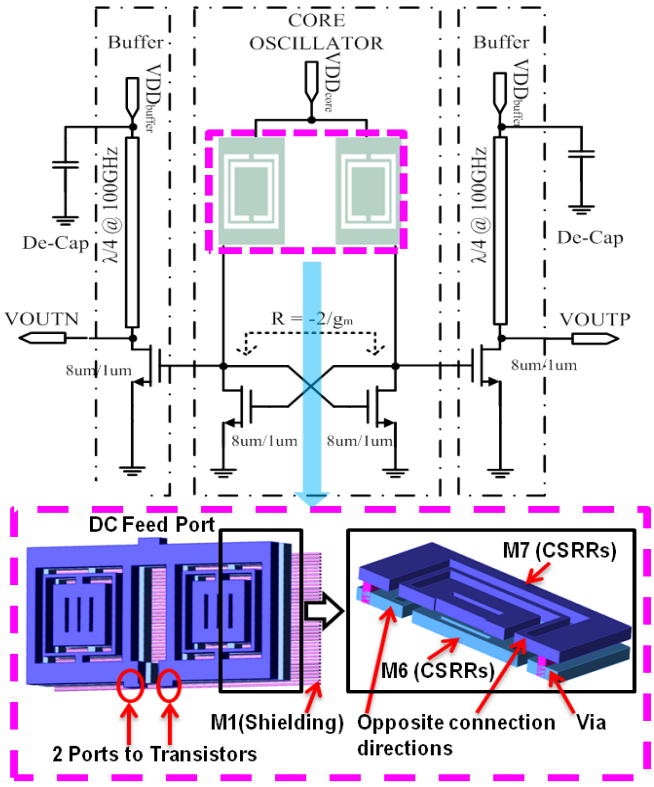


Fig. 4. Circuit diagram of the 96GHz CMOS oscillator with the use of the proposed metamaterial resonator by CSRR structure.

where *n* is the refractive index, *z* is the wave-impedance, *k* is wave-factor, and *d* is the physical length.

Based on (5), one can characterize the metamaterial resonator as follows. The proposed metamaterial resonator structure in Fig. 2(d) is implemented in STM65nm CMOS with resonance frequency biased around 100GHz. Its simulation results are shown in Fig. 3. ADS Momentum is used for the EM simulation to obtain the S-parameters. Extracted model parameters are: $L_1$=21pH, $L_2$=36pH, $C_1$=98fF, and $C_2$=67fF.

As shown in Fig. 3, a negative Re(ε) can be observed within a small band near the resonance frequency. As stated earlier, the negative Re(ε) and positive Re(μ) create the electric plasma, where propagating waves become evanescent waves [11]. As a result, energy cannot propagate through the resonator and are perfectly reflected backward. The deep rejection frequency band with a sharp cut-off can be viewed from $S_{12}$ plot in Fig.3, which means a high-Q performance of CSSR resonator.

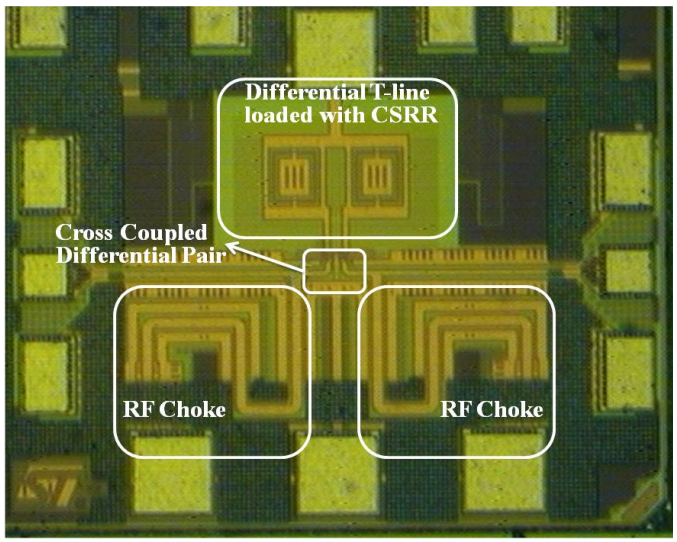


Fig. 5. Die photo of the fabricated 96GHz CMOS oscillator.

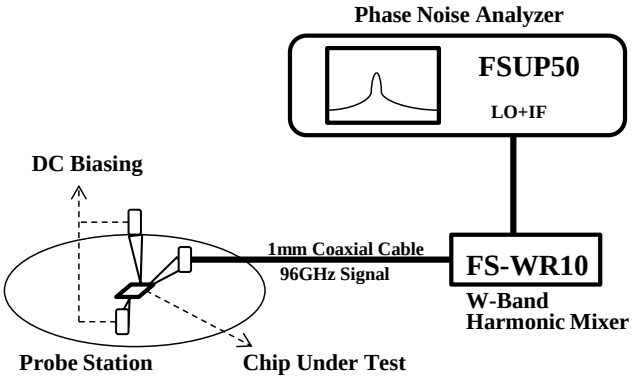


Fig. 6. Equipment setup for 100GHz phase noise measurement.

The Q-factor can be estimated with following equation [13]:

$$Q = \frac{f_0}{BW_{-3dB}} \tag{6}$$

where $f_0$ is the resonance frequency and $BW_{-3dB}$ is the bandwidth. With a $f_0$ of 102.5GHz and $BW_{-3dB}$ of 0.2GHz, the obtained Q-factor at resonance is 513.

## III. 96GHz Oscillator Implementation

To further demonstrate the high-Q performance of the proposed CSSR metamaterial resonator and its improvement in phase noise, a 96GHz oscillator is implemented in the same CMOS 65nm process (STM 7-metal-layer). The loss from the resonator is compensated by a cross-coupled pair of NMOS transistors, as shown in Fig. 4. To obtain the maximum $f_{MAX}$ with 65nm NMOS transistors, the individual finger width is designed to be 1um [1]. The total finger number is designed to be 8 to sustain the oscillation on slow-corner while minimizing parasitic capacitance.

In order to isolate the oscillator from the peripheral circuits and to provide enough output power for accurate phase noise

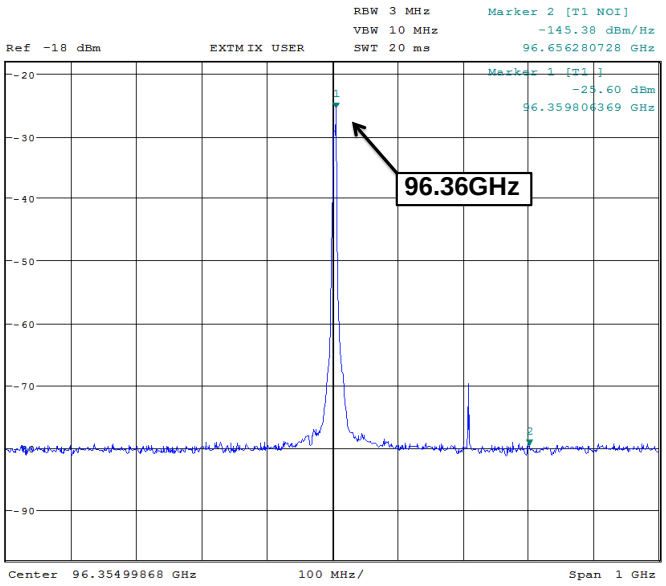


(a)

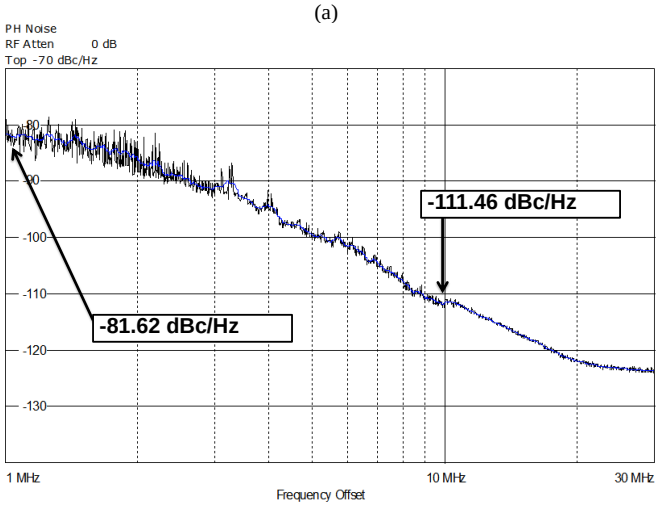


(b)

Fig. 7. Phase noise measurement results of the 96GHz oscillator by the proposed metamaterial resonator: (a) spectrum, and (b) phase noise.

measurement, the output is designed together with on-chip buffer and RF choke, which is composed of quarter-wavelength slow-wave T-line and de-coupling capacitor. All four transistors in the circuit are self-biased. The DC supply voltages for the core oscillator and buffer-stage are provided separately to identify the individual current consumption.

Note that the 1-metal-layer design of resonator used for demonstration in Fig. 1(c) is extended to a 2-metal-layer design during oscillator implementation with two CSRRs. The top and bottom CSRRs are implemented by M7 and M6, respectively. They are connected to DC feed port and output port in opposite directions, with vias to connect them together at both ends. Other than the benefit of size reduction, the stacked structure can improve the Q-factor, because the stacked two CSRRs are in the opposite directions thus forming a strong electric coupling between the 2 layers with confined the E-field. As such, the impact of the lossy substrate to the resonator Q-factor can be further reduced.

Moreover, the slow-wave shielding is implemented as well for further loss reduction. Note that the slow-wave shielding

TABLE I
STATE-OF-THE-ART 100GHZ OSCILLATOR PERFORMANCE COMPARISON

| **Parameters** | [14] | [15] | [16] | [17] | **This Work** | Unit |
|---|---|---|---|---|---|---|
| $f_{osc}$ | 104 | 128 | 100 | 122.5 | 96 | GHz |
| **VDD$_{core}$** | 1.48 | 1.2 | 1 | 0.8 | 1.2 | V |
| **Power$_{core}$** | 25.3 | 9 | 30 | 2 | 7.5 | mW |
| **Phase Noise @10MHz** | -105 | -105 | -110 | -103 | **-111.5** | dBc/Hz |
| **FOM** | -171.3 | -177.6 | -175.2 | 181.8 | **-182.4** | dBc/Hz |
| **Type** | Osc. | Osc. | VCO | VCO | Osc. | |
| **Tech.** | CMOS 130 | CMOS 90 | CMOS 90 | CMOS 65 | CMOS 65 | nm |

strips are designed by the bottom metal layer M1 with both width and pitch of 1um. The oscillator circuit is designed and verified with Agilent ADS Momentum for EM simulation and Cadence for oscillator circuit simulations.

## IV. MEASUREMENT RESULTS

The proposed CSRR-based metamaterial resonator is fabricated in 65nm CMOS process (STM 7-metal-layer). The die photo is shown in Fig. 5 with the area of 610um × 320um including RF PAD. As shown in Fig. 6, the RF and DC signals are connected through CASCADE Microtech Elite-300 probe station. The single-ended output of the chip is connected to phase-noise analyzer FSU-P50 from Rohde & Schwarz (R&S) for the phase noise measurement at MM-wave frequency region. To measure the signal frequency around 100GHz, W-band harmonic mixer FS-WR10 is used for down-conversion. Both the oscillator core and output buffer are supplied with 1.2V supply voltage, of which the current consumption is 6.24 mA and 6.53 mA, respectively. Thus the power consumption for oscillator core circuit is 7.5mW.

Fig. 7(a) shows the measured spectrum when the output frequency is 96.36 GHz, and the phase noise at this frequency is also shown in Fig. 7(b). One can observe that the phase noise is -111.5 dBc/Hz at 10MHz offset. Moreover, a widely used Figure of Merit (FOM) $L_{\Delta f} + 20\log(\Delta f/f_0) + 10\log(P/1mW)$ is employed, where $L_{\Delta f}$ is the measured phase noise at the offset frequency $\Delta f$ with respect to the fundamental oscillation frequency $f_0$, and $P$ is the DC power consumption of the core oscillator.

As described in Table I, the measurement results of the proposed 96GHz oscillator by CSSR-metamaterial based resonator show the state-of-the-art performance when compared to the recent oscillators designed at 100GHz using the traditional on-chip LC-tank resonators. Clearly, the proposed high-Q metamaterial resonator structure shows the best phase noise result of -111.5 dBc/Hz at 10MHz offset and FOM of -182.4 dBc/Hz at 96GHz.

## V. CONCLUSION

The application of high-Q metamaterial resonator constructed by the differential T-line loaded with CSRRs can effectively improve the phase-noise performance of CMOS on-chip oscillator at MM-wave frequency region. In this work, a 96GHz oscillator is designed and fabricated in CMOS 65nm process with the proposed CSSR-metamaterial based resonator structure. Measurement results show better phase noise performance when compared to the existing 100GHz oscillators by LC-tank based resonator. The state-of-the-art performance is demonstrated by CSSR-metamaterial based resonator with the phase noise of -111.5 dBc/Hz at 10MHz offset and FOM of -182.4 dBc/Hz. The future works have further demonstrated the use of CSSR oscillator in THz regenerative receiver and with the possible tuning feature.

## ACKNOWLEDGMENT

The authors would like to thank Mr. Lim Wei Meng from Nanyang Technological University and Mr. Cheong Iok Leong from R&S for the support of phase noise measurement.

## REFERENCES

[1] A. M. Niknejad and H. Hashemi, "mm-Wave Silicon Technology 60 GHz and Beyond," *Springer Science*, 2008.

[2] F. C. Commission, *E-band standard*, Federal Communication Commission Std., October 2003. [Online]. Available: http://fjallfoss.fcc.gov/edocs public/attachmatch/DOC-239368A1.pdf

[3] S. Kang, J.-C. Chien, and A. M. Niknejad, "A 100GHz phase-locked loop in 0.13um SiGe BiCMOS process," *RFIC Symposium*, pp. 1-4, June 2011.

[4] D. Cai, Y. Shang, H. Yu, J. Ren, "80GHz On-Chip Metamaterial Resonator by Differential Transmission Line Loaded with Split Ring Resonator", *IET Electronics Letter*, vol.48, no.18, pp.1128-1130, August 2012.

[5] R. A. Shelby, D. R. Smith, and S. Schultz, "Experimental Verification of a Negative Index of Refraction," *Science*, vol. 292, no. 5514, pp. 77–79, 2001.

[6] F. Falcone, T. Lopetegi, J. Baena, R. Marques, F. Martin, and M. Sorolla, "Effective negative- epsiv; stopband microstrip lines based on complementary split ring resonators," *IEEE Microwave and Wireless Components Letters*, vol. 14, no. 6, pp. 280 – 282, June 2004.

[7] C. G. Hwang and N. H. Myung, "Novel methods for phase noise reduction and harmonic suppression in a planar oscillator circuit based on split ring resonators," *APMC*, 2006.

[8] C. Lee, D. Jung, and C. Seo, "Design of low phase noise vco using complimentary split ring resonator," *APMC*, 2008.

[9] W. Fei, H. Yu, Y. Shang, and K. S. Yeo, "A 2D Distributed Power Combining by Metamaterial-based Zero-Phase-Shifter for 60GHz Power Amplifier in 65nm CMOS", *IEEE Transactions on Microwave Theory and Techniques*, 2013.

[10] A. Lai, T. Itoh, and C. Caloz, "Composite right/left-handed transmission line metamaterials," *IEEE Microwave Magazine*, vol. 5, pp. 34-50, Sept. 2004.

[11] T. J. Cui, D. R. Smith, and R. Liu, "Metamaterials: Theory, Design, and Applications," *Springer*, 2009.

[12] D. R. Smith, D. C. Vier, T. Koschny, and C. M. Soukoulis, "Electromagnetic parameter retrieval from inhomogeneous metamaterials," *Physical Review E*, vol. 71, p. 036617, 2005.

[13] J. Choi and C. Seo, "Novel low phase noise vco using high-Q metamaterial transmission line based on complementary spiral resonators," *IEEE Int. Microwave Symp. Dig.*, pp. 1501-1504, June 2009.

[14] O. Momeni and E. Afshari, "High Power Terahertz and Millimeter-Wave Oscillator Design: A Systematic Approach," *IEEE J. Solid-State Circuits*, vol. 46, pp. 583-597, Mar. 2011.

[15] B. Razavi, "A Millimeter-Wave Circuit Technique," *IEEE J. Solid-State Circuits*, vol. 43, pp. 2090-2098, Sept. 2008.

[16] L. M. Franca-Neto, R. E. Bishop, and B. A. Bloechel, "64 GHz and 100 GHz VCOs in 90 nm CMOS using optimum pumping method," *ISSCC Dig. Tech. Papers*, pp. 444-538 Vol.1, Feb. 2004.

[17] W. Volkaerts, M. Steyaert, and P. Reynaert, "118GHz fundamental VCO with 7.8% tuning range in 65nm CMOS," *IEEE RFIC Symposium*, pp. 1-4, June 2011.